

MONITORING OF SO₂ EMISSIONS FROM STACKS USING MULTISPECTRAL IMAGING IN THE UV AND VISIBLE SPECTRAL BANDS

E. Agassi, E. Hirsch

Israel Institute for Biological Research, P. O. Box 19, Nes Ziona 74100 – eyala@iibr.gov.il

KEY WORDS: Sulfur Dioxide, UV, EMCCD, Multispectral Imaging, Remote Sensing, Smoke Stack Emission,

ABSTRACT

Sulfur dioxide is one of the abundant pollutants in the modern world. It is mainly emitted due to the combustion of fossil fuels from both stationary and mobile sources. Such emissions may produce heavy pollution over vast areas with noticeable adverse health effects. Therefore, it is important to maintain monitoring of the major stationary sources (such as power plants) that emit SO₂, of rates of few hundreds of kilograms per hour. Remote sensing of the emitted SO₂ plumes is a useful way to monitor these emissions continuously and accurately, without relying on the cooperation of the industrial facilities that operate the stacks. FTIR measurements offer a well established technique for such monitoring, but since they are carried in the long wave infrared, knowledge of the emission temperature is essential in order to extract the true concentration of the pollutant. On the other hand, monitoring in the UV spectral band eliminates this drawback and can employ the higher absorbance of SO₂ in this band. In this article we present SO₂ monitoring in the UV band using multispectral imaging based on EMCCD and narrow band filters. Multispectral imaging is necessary to validate that the emitted pollutant is indeed SO₂ and not soot particles or other pollutants such as NO₂. The imaging capability enables efficient background removal that, in turn, yields an accurate extraction of the concentration-length (CL) value of the plume. Implementation of the suggested monitoring method is demonstrated using data collected from field measurements.

1. INTRODUCTION

Sulfur dioxide (SO₂) is a colorless gas with a sharp and irritating odor. It is toxic gas, with significant environmental impact and adverse effects on human health (EPA web site). Natural sources of sulfur dioxide include releases from volcanoes, oceans, and biological decay and forest fires. Of them, erupting volcanoes account for a significant amount of SO₂ emissions (Sigurdsson, 2000), ~50% of the SO₂ in the Earth's atmosphere. SO₂ is a major pollutant to the Earth's atmosphere and affects human health when excessively inhaled, it creates acid rain that destroys buildings and metal structures.

The main artificial stationary sources of SO₂ releases into the atmosphere are emissions from smoke stacks of combusted fossil fuel – mainly heavy fuel and coal. Other sources are catalytic cracking and sulfur recovery facilities in refineries, smelting of mineral ores that contain the sulfur species in the form of sulfates and sulfides and sulfur acid production plants (Davis, 2000). Electric power plants, refineries and other large scale chemical plants that consume high amounts of energy release high quantities of SO₂ into the atmosphere. For example – combustion of heavy fuel that contains 1% sulfur yields an emission of 1750 mg/Nm³ of SO₂ at the stack

outlet. According to the EPA, power plants fed by coal, oil and natural gas release 13, 12 and 1.7 lbs/MWh of Sulfur dioxide gas respectively (EPA web site). When the industrial facilities are dense and located in an area with frequent bad atmospheric conditions (such as an existence of low altitude inversion layer), a constant monitoring of the SO₂ emissions is critical to avoid noticeable and dangerous increases in ground level concentrations. In such cases, plants can be regulated to feed the combustion with low concentration sulfur fuel in order to reduce the emitted SO₂ amounts respectively. However, this regulation can't be validated independently from the monitored data supplied by the plants themselves. Hence remote sensing of the emitted sulfur dioxide concentrations can be employed as an effective method to enforce the emission standards without a need for a corporation from the monitored plant. Sulfur dioxide molecule has two intense absorption bands that can be employed for remote sensing – at the UV and at the LWIR spectral bands (Figure 1).

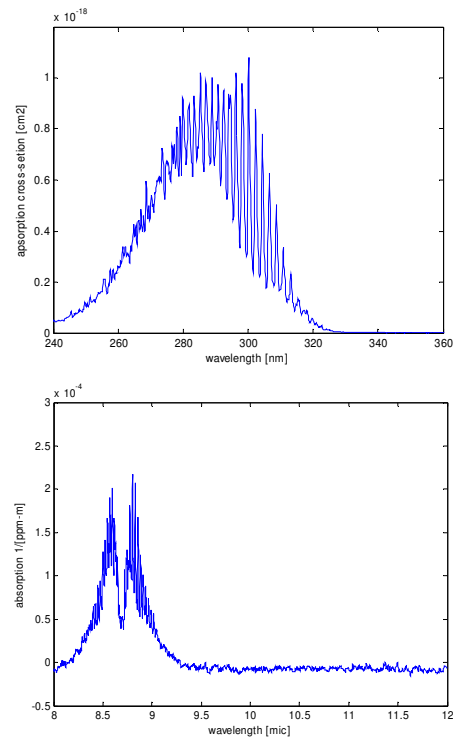


Figure 1. The absorbance of SO₂ vapor in the UV (up – after Bogumil et al. 2003) and the LWIR (down – after Hanst).

While the first is an order magnitude more intense than the other, its use has some drawbacks:

1. Remote monitoring can be conducted only during daylight hours.
2. Most of the strong absorption is within the solar blind spectral band and poor background illumination.
3. Low atmospheric visibility limits the sensing range.

However, the advantages of utilizing this band are the strong absorption and detection thresholds independent on temperature contrast.

Remote sensing of SO₂ released from volcanoes is routinely carried out both in the IR and the UV spectral band (Bluth et al. 2007, Kantzas et al. 2008, Watson et al. 2004, Amici et al. 2007). However, remote sensing of the effluent sulfur dioxide plumes from combustion stacks is usually done only by ground based non-imaging IR spectroscopy (such as FTIR) (Mattu et al. 2000, Chaffin et al. 2001), or by off source down wind

measurements (McGogigle et al. 2004). UV spectroscopy is also used, but usually for off source monitoring, or for measurements of outdoor concentrations (such as the technique of differential optical absorption sensing - DOAS) or inside the stack duct (reference No. 14).

First attempts at SO₂ monitoring with a UV camera were carried out in the 1960's. Until recently, another disadvantage of the UV spectral band had been the lack of suitable imaging sensors with narrow band-pass filters that can provide high quality images at long exposures at the upper edge of the solar blind spectral band. However, the recent availability of EMCCD (Holst and Lomheim) sensors provides an efficient and sensitive tool for remote sensing of SO₂ plumes emitted from stationary sources.

This article introduces a novel technique for the monitoring of effluent SO₂ emissions from stacks using the advantages of EMCCD technology. The tools presented throughout this article can be extended for monitoring other gaseous pollutants in the visible-UV spectral range, such as NO₂, CS₂, Cl₂, and Br₂, and can be also modified for monitoring in the IR spectral band as well.

2. EXPERIMENTAL

2.1 Measurements Sensor

Smoke stack emissions were measured with an EMCCD imager called Sensicam (PCO AG, Germany). The collective UV quartz optics was a fixed 105mm focal length lens (F_#=4, manufactured by Goyo Optical, Inc., Japan) with one of three custom made narrow band pass filters and one cut-on filter (Omega® Optical, Inc. USA), as specified in table 1.

Band #	Spectral Range [nm]	Aim
1	295-315	SO ₂ emissions monitoring
2	320-340	Cl ₂ , CS ₂ emissions elimination
3	380-420	Br ₂ , NO ₂ emissions elimination
4	780+	Clear reference

Table 1. The spectral band pass transmission of the four filters used in our measurements. Band wavelengths limits refer to 50% of peak transmission. Out band rejection is better than 1E-4.

The spectral transmissions of the filters were chosen to ensure that we indeed sense the SO₂ plume, as explained below. Figure 2 shows the absorption spectra of other common pollutants in the UV-visible band. Using only a single filter might lead to misinterpretation of high concentration-lengths of other compounds rather than SO₂. Therefore, band 2 and 3 are used for eliminating the possibilities of CS₂, Cl₂ and NO₂, Br₂ emissions, respectively. The wide NIR band is used as a clear reference for all the gaseous emissions. Figure 3 explains why a high integration time, reduced dark current and large well depth are needed for effective SO₂ monitoring – the spectral range with the highest absorption is adjoined by very poor background illumination.

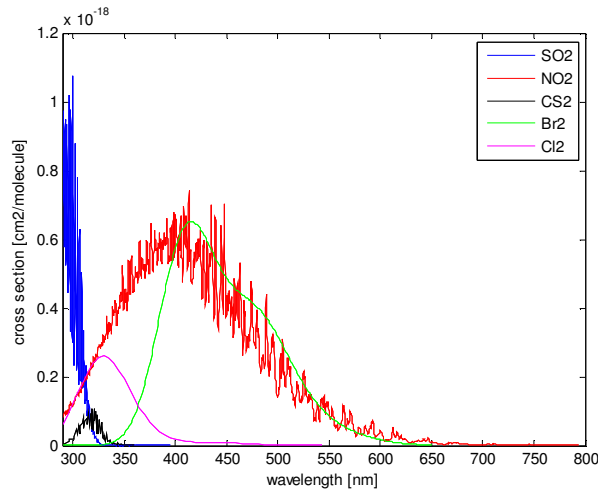


Figure 2. The absorption spectra of sulfur dioxide and other common pollutants in the UV and visible spectral bands (after references – (Bogumil et al. 2003, Vandaele et al. 1998, Wine et al. 1981, Tellinghuisen 2003, Hubinger and Nee 1995).

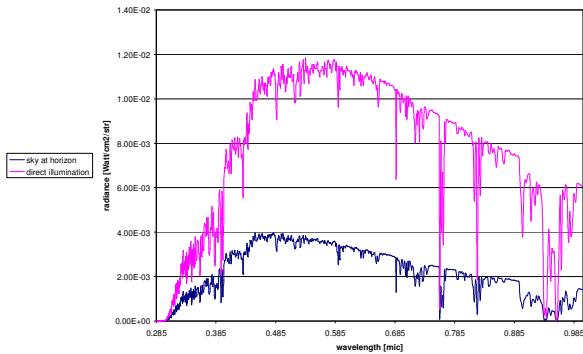


Figure 3. The background illumination (of terrain with 30% reflectance and of low angle sky - all calculated by MODTRAN with 23km visibility range) near the main absorption band of SO₂.

2.2 Data Gathering

Data collection was carried out at a large petrochemical complex which includes a refinery and adjacent industries. Each stack emission was measured with all the band pass filters sequentially, and the obtained images were recorded on a PC hard disk. The weather was fair during the measurements with variable amounts of high altitude clouds. A typical multispectral image is shown in figure 4 (The integration times in band 1 varied

between 1-8 seconds, but since the sources are stationary – that long exposure was not a concern).

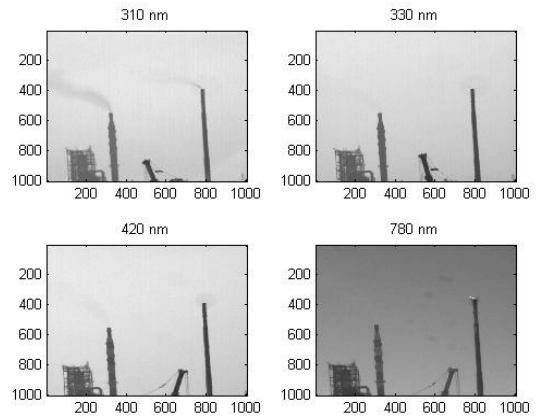


Figure 4. A typical multispectral image of smoke stack emission at a large petrochemical compound.

3. DATA PROCESSING

The aim of the data processing was to extract the SO₂ transmission in each band and to verify that the one obtained in the first band is much lower than those obtained in the other bands. Neglecting atmospheric effects, we can write the following term for the plume signal within the band j and at every pixel location (x, y) :

$$I_j = \int_0^{\infty} I_B(\lambda) \exp(-\alpha(\lambda)CL) f_j(\lambda) d\lambda \quad (1)$$

Where:

$f_j(\lambda)$ - Sensor spectral response (QE, optics, filter transmission) at spectral band j .

$I_B(\lambda)$ - Background illumination beyond the plume at location (x, y) .

$\alpha(\lambda)$ - The mass extinction coefficient (pure absorption) of SO₂ vapor at a wavelength λ .

CL – The concentration-length of the plume at location (x, y) .

The explicit dependence upon the location was omitted in eq. (1). Another simplification is performed by using the term CL instead

of $\int_0^{\infty} C(r)dr$. It can be justified, at least near

the stack outlet, where the concentration is fairly uniform and the plume width is approximately the stack's diameter D (Gellison 2004, Gellison et al. 2003). If the spectral properties of the clear background, sensor's response and the stack diameter are known, we can extract the SO_2 concentration as emitted from the stack.

The weighted plume transmission at each spectral band can be obtained by dividing eq. (1) by the clear background signal:

$$\bar{\tau}_j = \frac{\int_0^{\infty} I_B(\lambda) \exp(-\alpha(\lambda)CL) f_j(\lambda) d\lambda}{\int_0^{\infty} I_B(\lambda) f_j(\lambda) d\lambda} \quad (2)$$

Note that due to the sharp dependence of I_B and α upon the wavelength (figures 2-3), we cannot extract the true concentration-length without a pre-calibration of the sensor. It can be done either by collecting a training set of data and comparing it to in-situ measurements in the stack duct, or by estimating the spectral distribution of the clear background.

Observation from a distance adds atmospheric effects to the obtained signal. Let us assume that the stack's background is low angle sky – i.e.:

$$I_B(\lambda) = A(\lambda) \quad (3)$$

where $A(\lambda) = \int_0^{\infty} I_{path}(\lambda; r) dr$ is the integral

over the path scattered radiance.

Monitoring the stack from a distance of R results in degradation of the effective plume transmittance and it becomes:

$$\bar{\tau}_j(R) = 1 - \frac{\int_0^{\infty} A(\lambda) \tau_a(\lambda; R) [1 - \exp(-\alpha(\lambda)CL)] f_j(\lambda) d\lambda}{\int_0^{\infty} A(\lambda) f_j(\lambda) d\lambda} \quad (4)$$

Where $\tau_a(\lambda; R)$ is the atmospheric extinction at a range of R and a wavelength λ . Hence, eliminating path radiance effect is essential when considering monitoring from long distances.

The crucial processing step is the estimation of the clear background beyond the plume. For this estimate we use the advantage of an imaging sensor:

First, the user defines a polygon that encloses the plume (left hand side of figure 5).

Second, we estimate the background inside the polygon using the built in method "roifill" of MATLAB® software. This method performs a smooth interpolation into the polygon by using the pixel values on its boundary, in such a manner that every pixel equals the average value of its neighbors.

Since the sky background has a very smooth texture the obtained background estimation has good accuracy (right hand side of figure 5).

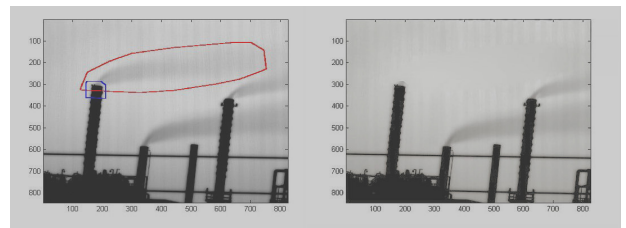
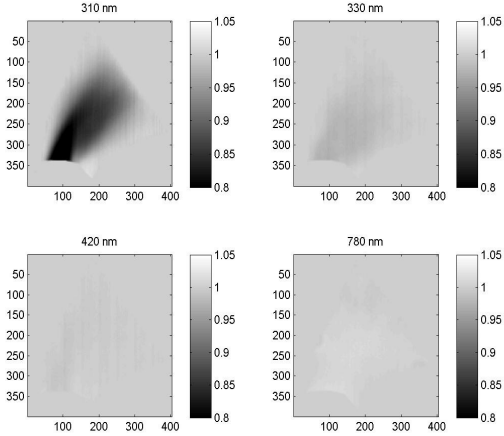


Figure 5. On the left hand side: a typical polygon that defines the locus of the plume. In order to avoid inserting unrelated values into the interpolation process of the sky polygon, a second polygon was defined (marked in blue) that excludes the stack area from the boundary of the sky polygon. On the right hand side: The clear sky background estimation inside the polygon defined on the left side of this figure.

Knowing the clear background enables us to calculate the transmission in each pixel (inside the area bounded by the polygon) according to eq. (2). The results are presented in figures 6-7.



ERROR: stackunderflow
OFFENDING COMMAND: ~

STACK: